Inorganic Chemistry

Article

pubs.acs.org/IC

Structural Origin of the Anisotropic and Isotropic Thermal Expansion of K_2NiF_4-Type $LaSrAlO_4$ and Sr_2TiO_4

Keishi Kawamura,[†] Masatomo Yashima,*[,†] Kotaro Fujii,[†] Kazuki Omoto,[‡] Keisuke Hibino,[†] Shuntaro Yamada,[†] James R. Hester,[§] Maxim Avdeev,[§] Ping Miao,[#] Shuki Torii,[#] and Takashi Kamiyama[#,⊥]

[†]Department of Chemistry and Materials Science, Graduate School of Science and Engineering and [‡]Department of Materials Science and Engineering, Interdisciplinary Graduate School of Science and Engineering, Tokyo Institute of Technology, 2-12-1-W4-17, O-okayama, Meguro-ku, Tokyo 152-8551, Japan

[§]Bragg Institute, Australian Nuclear Science and Technology Organisation, Locked Bag 2001, Kirrawee DC, NSW 2232, Australia

[#]Neutron Science Laboratory, Institute of Materials Structure Science, High Energy Accelerator Research Organization (KEK), 1-1 Oho, Tsukuba, Ibaraki 305-0801, Japan

[⊥]The Graduate University for Advanced Studies (SOKENDAI), SOKENDAI-KEK Office, 1-1 Oho, Tsukuba, Ibaraki 305-0801, Japan

Supporting Information

ABSTRACT: K_2NiF_4-type $LaSrAlO_4$ and Sr_2TiO_4 exhibit anisotropic and isotropic thermal expansion, respectively; however, their structural origin is unknown. To address this unresolved issue, the crystal structure and thermal expansion of $LaSrAlO_4$ and Sr_2TiO_4 have been investigated through high-temperature neutron and synchrotron X-ray powder diffraction experiments and ab initio electronic calculations. The thermal expansion coefficient (TEC) along the c-axis (α_c) being higher than that along the a-axis (α_a) of $LaSrAlO_4$ [$\alpha_c = 1.882(4)\alpha_a$] is mainly ascribed to the TEC of the interatomic distance between Al and apical oxygen O2 α(Al−O2) being higher than that between Al and equatorial oxygen O1 α(Al−O1) [α(Al−O2) = 2.41(18)α(Al−O1)]. The higher α(Al−O2) is attributed to the Al−O2 bond being longer and weaker than the Al−O1 bond. Thus, the minimum electron density and bond valence of the Al−O2 bond are lower than those of the Al−O1 bond. For Sr_2TiO_4, the Ti−O2 interatomic distance, d(Ti−O2), is equal to that of Ti−O1, d(Ti−O1) [d(Ti−O2) = 1.0194(15)d(Ti−O1)], relative to $LaSrAlO_4$ [d(Al−O2) = 1.0932(9)d(Al−O1)]. Therefore, the bond valence and minimum electron density of the Ti−O2 bond are nearly equal to those of the Ti−O1 bond, leading to isotropic thermal expansion of Sr_2TiO_4 than $LaSrAlO_4$. These results indicate that the anisotropic thermal expansion of K_2NiF_4-type oxides, A_2BO_4, is strongly influenced by the anisotropy of B−O chemical bonds. The present study suggests that due to the higher ratio of interatomic distance $d(B-O2)/d(B-O1)$ of $A_2^{2.5+}B^{3+}O_4$ compared with $A_2^{2+}B^{4+}O_4$, $A_2^{2.5+}B^{3+}O_4$ compounds have higher $\alpha(B-O2)$, and $A_2^{2+}B^{4+}O_4$ materials exhibit smaller $\alpha(B-O2)$, leading to the anisotropic thermal expansion of $A_2^{2.5+}B^{3+}O_4$ and isotropic thermal expansion of $A_2^{2+}B^{4+}O_4$. The "true" thermal expansion without the chemical expansion of A_2BO_4 is higher than that of ABO_3 with a similar composition.

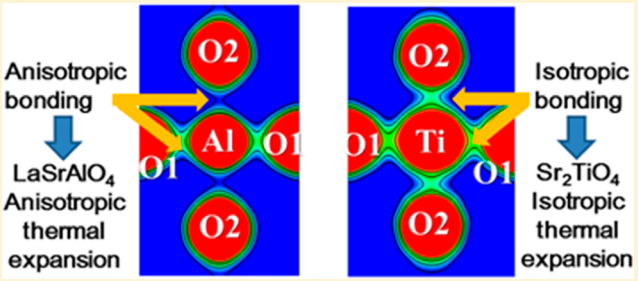

1. INTRODUCTION

The crystal structure of a K_2NiF_4-type oxide A_2BO_4, such as $LaSrAlO_4$ and Sr_2TiO_4, consists of the alternate stacking of rock-salt AO- and perovskite ABO_3-layers (Figure 1). Here, A and B are larger and smaller cations, respectively. The K_2NiF_4-type oxides exhibit a variety of interesting electrical and magnetic properties.[1−4] Because of these properties, K_2NiF_4-type materials have attracted considerable attention as electrode materials in solid oxide fuel cells (SOFCs),[5−11] oxygen separation membranes,[9−11] high-T_c superconductors,[12] substrates for thin films of high-T_c superconductors,[13,14] and lasers.[15] Thermal expansion and its anisotropy in ceramic materials are critical for the thermomechanical stability of SOFCs,[16−19] crystal growth, and residual stresses in epitaxial films.[13,20] If the mismatch in thermal expansion between membranes is significant, it will induce stresses during thermal cycling, leading to cracks and delamination.[21] The anisotropy of thermal expansion of K_2NiF_4-type oxides depends on the chemical composition. Many K_2NiF_4-type oxides, such as $LaSrAlO_4$,[22,23] La_2NiO_4,[24] $La_{2-x}Sr_xFeO_{4+\delta}$,[25] $Pr_2(Ni_{0.75}Cu_{0.25})_{0.95}Ga_{0.05}O_{4+\delta}$,[26] $La_{2-x}Sr_xMnO_4$,[27] $CaNdAlO_4$,[22] $CaErAlO_4$,[28] and $CaYAlO_4$[29], exhibit anisotropic thermal expansion, whereas the thermal expansion of some K_2NiF_4-type materials, such as Sr_2TiO_4[30,31] and Sr_2SnO_4[32], is relatively isotropic. Here, x and δ are the contents of Sr and excess oxygen, respectively. For example, in

Received: January 14, 2015
Published: April 2, 2015

DOI: 10.1021/acs.inorgchem.5b00102
Inorg. Chem. 2015, 54, 3896−3904

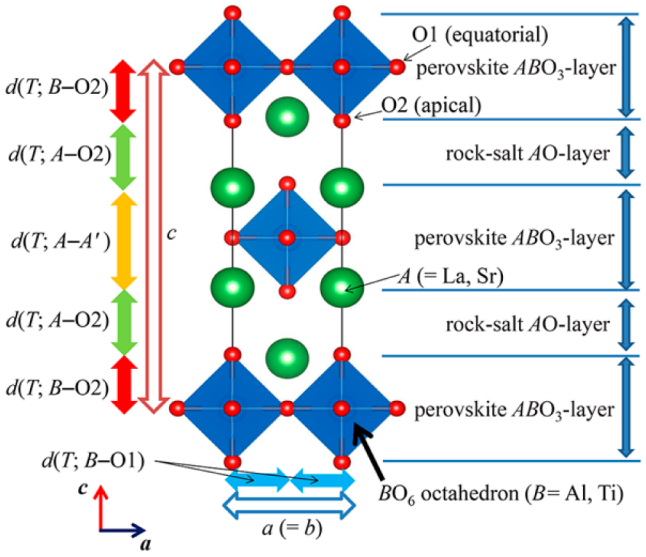

Figure 1. Crystal structure of K_2NiF_4-type tetragonal $I4/mmm$ A_2BO_4 ($LaSrAlO_4$ and Sr_2TiO_4) depicted with BO_6 octahedra (blue squares), A cations (green spheres), and O anions (red spheres). The relationships between the unit-cell parameters and interatomic distances are shown.

$LaSrAlO_4$, the average thermal expansion coefficient along the c-axis ($\alpha_c = (1.71–1.9) \times 10^{-5}$ K^{-1}) is higher than that along the a-axis ($\alpha_a = (0.755–0.89) \times 10^{-5}$ K^{-1}) ($\alpha_c > \alpha_a$).[22,23] In contrast, the thermal expansion of Sr_2TiO_4 is relatively isotropic ($\alpha_c = 1.44 \times 10^{-5}$ $K^{-1} \approx \alpha_a = 1.46 \times 10^{-5}$ K^{-1}).[30,31] However, the atomic-scale structural origin of the anisotropic and isotropic thermal expansions of the K_2NiF_4-type oxides is poorly understood. Furthermore, in many K_2NiF_4-type $A_2BO_{4+\delta}$ oxides (B = Co, Ni, Cu, Mn, and Fe),[24−27] the valence of the B cation increases and oxygen content δ decreases with increasing temperature, which yields chemical expansion in addition to the "true" thermal expansion. Most previous studies have not quantitatively examined the relationship between the thermal expansion and the temperature dependence of interatomic distances in K_2NiF_4-type materials. Thus, Omoto et al. studied the crystal structure and thermal expansion of $CaErAlO_4$[28] and $CaYAlO_4$[29] without chemical expansion. However, the reason that anisotropy in thermal expansion depends on atomic species A and B is unknown. To address this important question, in this study, we have chosen to use the chemicals $LaSrAlO_4$ and Sr_2TiO_4, because $LaSrAlO_4$ and Sr_2TiO_4 exhibit (i) anisotropic and isotropic thermal expansion, respectively, and (ii) very little chemical expansion, which enables the investigation of "true" thermal expansion without interference from chemical expansion. The first aim of the present work is to examine the structural origin of anisotropic thermal expansion in $LaSrAlO_4$ and of isotropic thermal expansion in Sr_2TiO_4 through the temperature dependence of interatomic distances obtained by Rietveld analysis of high-temperature neutron powder diffraction data from 298 to 1273 K. In this work, the high-temperature neutron-diffraction technique was utilized because this method allows accurate determination of atomic coordinates of a relatively light element (oxygen) in complex oxides kept at a high temperature.[33,34] Here, the accurate atomic coordinates of oxygen atoms in $LaSrAlO_4$ and Sr_2TiO_4 are essential to the determination of cation−anion distances, which are of vital importance for the atomic-scale structural origin of anisotropic and isotropic thermal expansion. The thermal expansion of interatomic distance (bond length) can be discussed in terms of electron-density distribution[26,28,29] and bond valence.[35,36] However, the thermal expansion of interatomic distances in K_2NiF_4-type oxides has not been studied through their bond valences. The second aim of this work is to examine the electron-density distribution and bond valence and to discuss the origin of the anisotropic and isotropic thermal expansion of Al−O and Ti−O bond lengths and cell parameters in $LaSrAlO_4$ and Sr_2TiO_4.

2. EXPERIMENTAL AND CALCULATION SECTION

Synthesis. $LaSrAlO_4$ and Sr_2TiO_4 samples were synthesized by the solid-state-reaction method. For $LaSrAlO_4$, the starting materials were high-purity (>99.9%) powders of La_2O_3, $SrCO_3$, and Al_2O_3. To remove water content, La_2O_3 was heated at 1000 °C for 10 h. These powders were weighed in stoichiometric ratios and mixed for ∼1 h in an agate mortar. This mixture was calcined at 1000 °C for 10 h and ground for ∼1 h in the agate mortar. Then, it was pressed into pellets at ∼50 MPa and then sintered in air at 1400 °C for 12 h. The sintered products were crushed in a WC mortar, ground in the agate mortar, and then sintered in air at 1400 °C for 12 h. Sr_2TiO_4 was also prepared by the solid-state-reaction method. Stoichiometric amounts of $SrCO_3$ and TiO_2 (>99.9% purity) were mixed for ∼1 h in the agate mortar and calcined in air at 1000 °C for 10 h. After grinding, the mixture was pressed into pellets and sintered in air at 1100 °C for 12 h. The cation chemical compositions were confirmed by inductively coupled plasma optical emission spectroscopy (ICP-OES). The weight change was examined by thermogravimetric analysis (TGA), where the heating and cooling rates were 10 K min^{-1}.

Crystal Structure Refinements and MEM Electron-Density Analysis. Neutron powder diffraction measurements of $LaSrAlO_4$ and Sr_2TiO_4 were performed in situ between 298 and 1273 K with constant-wavelength neutrons of 1.62137(4) Å (step interval: 0.1°/2θ). The samples were heated with a vacuum furnace under 10^{-4} Pa, and the diffraction measurements were carried out on the angle-dispersive-type neutron diffractometer Echidna[37] at the Open Pool Australian Light water reactor (OPAL) at the Bragg Institute, Australian Nuclear Science and Technology Organisation (ANSTO). Neutron-diffraction data of Sr_2TiO_4 were also measured by time-of-flight (TOF) neutron powder diffractometers SuperHRPD (BL08)[38] from room temperature (RT) to 1073 K and iMATERIA (BL20)[39] at RT at the Material and Life Science Facility (MLF) of the Japan Proton Accelerator Research Complex (J-PARC). Synchrotron X-ray powder diffraction measurements were carried out at 300 K using a Debye−Scherrer camera with an imaging plate detector installed at the BL19B2 experimental station of SPring-8, Hyogo, Japan.[40] Synchrotron X-rays with a wavelength of 0.399712(2) Å were used for the measurements with a step interval of 0.01°/2θ. The Echidna and synchrotron diffraction data were analyzed by the Rietveld method with the computer program RIETAN-FP,[41] whereas the TOF neutron data were analyzed by Z-Rietveld (Windows Ver. 0.9.42.4).[42] The experimental electron-density distribution at 300 K was obtained by a combination technique of Rietveld analysis and the maximum-entropy method (MEM) for the synchrotron X-ray powder diffraction data. The MEM analysis was carried out with the program Dysnomia[43] (128 × 128 × 384 pixels). The crystal structure and electron-density distribution were visualized by the VESTA program.[44]

Ab Initio Electronic Calculations. The theoretical electron-density distribution was studied by ab initio electronic calculations based on the density functional theory (DFT) with the VASP code.[45] We used 1 × 1 × 1 cells $(LaSrAlO_4)_2$ and $(Sr_2TiO_4)_2$ for the DFT calculations. Calculations were performed using projector augmented-wave (PAW) potentials for Sr, La, Al, Ti, and O atoms and a plane-wave set with a cutoff of 500 eV. The calculations were carried out by the Perdew−Burke−Ernzerhof (PBE) generalized gradient approximation (GGA) for the exchange and correlation functionals. The electronic iteration convergence was set to 10^{-8} eV. Sums over occupied electronic states were performed using the Monkhorst−Pack scheme on a 7 × 7 × 3 set of the k-point mesh. The unit-cell and positional parameters were optimized with the convergence condition of 0.001 eV $Å^{-1}$. For $LaSrAlO_4$, all three models with different Sr and La atomic distributions

DOI: 10.1021/acs.inorgchem.5b00102
Inorg. Chem. 2015, 54, 3896−3904

over the positions in the perovskite and rock-salt blocks were investigated, and they gave similar electron-density distributions.

3. RESULTS AND DISCUSSION

Figures 2 and 3 show the neutron and synchrotron X-ray powder diffraction profiles of $LaSrAlO_4$ and Sr_2TiO_4 samples. Between

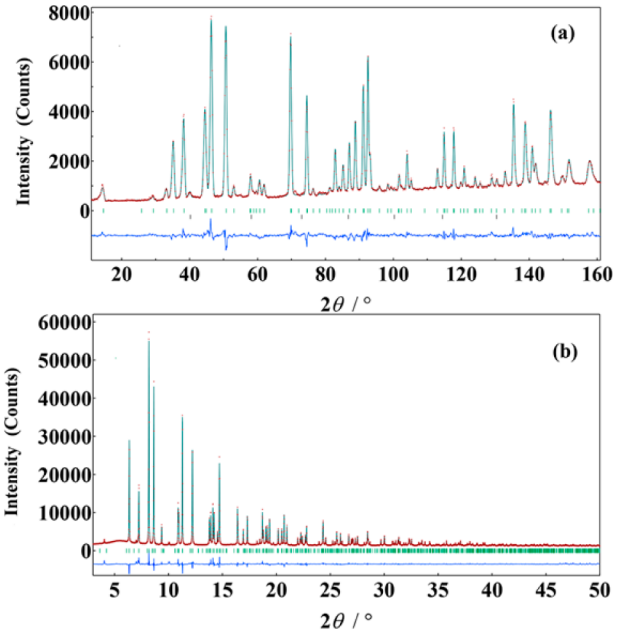

Figure 2. Rietveld patterns of (a) neutron and (b) synchrotron X-ray powder diffraction data of $LaSrAlO_4$ measured at (a) 1273 K and (b) 300 K. Red plots denote observed data, the green line denotes calculated profiles, and the blue line denotes the difference. Vertical lines indicate possible Bragg peaks of $LaSrAlO_4$ (green) and Nb from the furnace (black).

298 and 1273 K, they were identified as a tetragonal phase with the $I4/mmm$ K_2NiF_4-type structure (Figure 1) in addition to very weak peaks of niobium from the furnace. In preliminary Rietveld analyses, the refined occupancy factor of oxygen atoms was unity within 3σ at the maximum temperature 1273 K, where σ is the estimated standard deviation (see Supporting Information). Furthermore, there was very little weight loss during heating as evidenced by thermogravimetric analysis (TGA, Figure S1 in the Supporting Information). Therefore, in the final refinements, we fixed the occupancy factor of oxygen atoms to unity. These results indicate that there is no change in the valence of constituent cations and oxygen content during the high-temperature neutron diffraction measurements. Thus, we are able to study the "true" thermal expansion without chemical expansion in the present work. The refined crystallographic parameters are shown in Tables 1 and 2. The calculated profiles are in good agreement with the observed intensities (Figures 2 and 3). The unit-cell and positional parameters obtained from neutron diffraction data measured by the Echidna diffractometer at 298 K agree with those from synchrotron X-ray diffraction data at 300 K, from TOF SuperHRPD and iMATERIA neutron data at RT, and from DFT calculations. The present refined crystal parameters of $LaSrAlO_4$ and Sr_2TiO_4 are consistent with those presented in the literature.[46,47] For $LaSrAlO_4$ (A = La,Sr and B = Al), the B−(apical oxygen atom O2) distance, $d(B-O2)$ (2.0535(16) Å) is longer than that of B−(equatorial oxygen atom O1) (1.87832(3) Å) (B = Al): $[d(B-O2)/d(B-O1) = 1.0932(9) > 1]$. For Sr_2TiO_4 (A = Sr and B = Ti), the B−O2 distance (1.981(3) Å) is nearly equal to that of B−O1 (1.94328(4) Å): $[d(B-O2)/d(B-O1) = 1.0194(15)]$. In general, the ratio of interatomic distance $d(B-O2)/d(B-O1)$ of K_2NiF_4-type $A_2^{2.5+}B^{3+}O_4$, including $LaSrAlO_4$ (1.09−1.20), is higher than that of $A^{2+}{}_2B^{4+}O_4$, including Sr_2TiO_4 (0.98−1.03).[48]

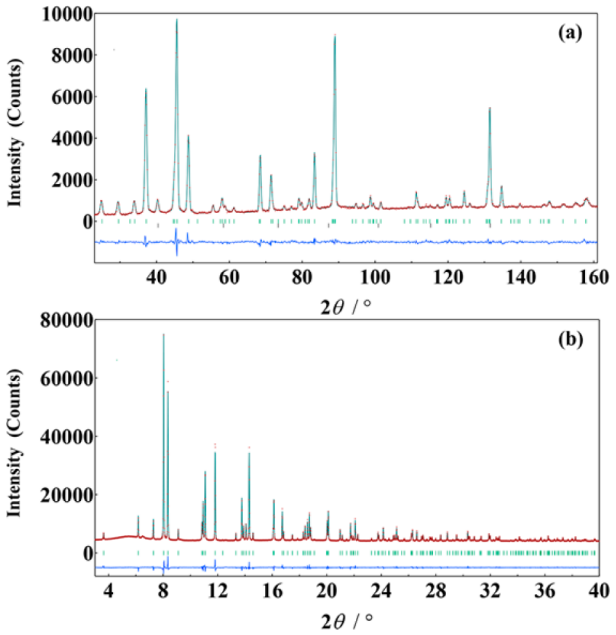

Figure 3. Rietveld patterns of (a) neutron and (b) synchrotron X-ray powder diffraction data of Sr_2TiO_4 measured at (a) 1273 K and (b) 300 K. Red plots denote observed data, the green line denotes calculated profiles, and the blue line denotes the difference. Vertical lines indicate possible Bragg peaks of Sr_2TiO_4 (green) and Nb from the furnace (black).

$$d(B-O2)/d(B-O1) = 1.09 \sim 1.20 > 1 \text{ for } A_2{}^{2.5+}B^{3+}O_4 \quad (1)$$

$$d(B-O2)/d(B-O1) = 0.98 \sim 1.03 \approx 1 \text{ for } A_2{}^{2+}B^{4+}O_4 \quad (2)$$

The different values of the $d(B-O2)/d(B-O1)$ ratios between $A_2{}^{2.5+}B^{3+}O_4$ and $A_2{}^{2+}B^{4+}O_4$ can qualitatively be explained by the multiscale minimization of the electric polarization.[49] Here, $A^{2.5+}$ is a cation with an average formal valence of +2.5, which is larger than the B^{3+} cation.

Next, we describe the temperature dependence of the crystal structure of $LaSrAlO_4$ and Sr_2TiO_4, which were obtained by Rietveld analysis of the Echidna neutron data. The results of Sr_2TiO_4 from the SuperHRPD neutron data were in good agreement with those from the Echidna data. The unit-cell parameters a and c, unit-cell volume, and atomic displacement parameters of $LaSrAlO_4$ and Sr_2TiO_4 increase with temperature (Tables 1 and 2 and Figures S2 and S3 in the Supporting Information). The thermal expansions $\Delta a/a_0$ and $\Delta c/c_0$ also increase with temperature (Figure 4). Here, $\Delta a/a_0$ and $\Delta c/c_0$ are defined as $\Delta a/a_0 \equiv [a(T) - a(298)]/a(298)$ and $\Delta c/c_0 \equiv [c(T) - c(298)]/c(298)$, respectively, and $a(T)$ and $c(T)$ are the unit-cell parameters a and c at temperature T (K). For $LaSrAlO_4$, $\Delta c/c_0$ is higher than $\Delta a/a_0$ at a high temperature, whereas $\Delta c/c_0$ is nearly equal to $\Delta a/a_0$ for Sr_2TiO_4. The average thermal expansion coefficients (TECs) along the a- and c-axes between 298 and 1273 K are defined as

DOI: 10.1021/acs.inorgchem.5b00102
Inorg. Chem. 2015, 54, 3896−3904

Table 1. Refined Crystallographic Parameters and Reliability Factors in the Rietveld Analysis of $LaSrAlO_4$ at Different Temperatures[a] and Crystallographic Parameters Optimized by DFT Calculations[b]

method		neutron diffraction through the Echidna diffractometer[a]						synchrotron[a]	DFT[b]
temperature		298 K	473 K	673 K	873 K	1073 K	1273 K	300 K	
	$a = b$ (Å)	3.75664(3)	3.76424(4)	3.77008(4)	3.77582(4)	3.78356(4)	3.79118(5)	3.75577(3)	3.76672
	c (Å)	12.6439(2)	12.6971(3)	12.7338(3)	12.7719(3)	12.8175(3)	12.8627(2)	12.63269(11)	12.90146
La,Sr	z	0.35837(9)	0.35844(11)	0.35864(11)	0.35879(11)	0.35908(12)	0.35907(12)	0.35880(4)	0.3570
	U_{iso} (Å^2)	0.0044(2)	0.0079(3)	0.0111(3)	0.0110(3)	0.0131(3)	0.0171(3)	0.00492(10)	
Al	$U_{11} = U_{22}$ (Å^2)	0.0009(7)	0.0011(9)	0.0030(9)	0.0041(9)	0.0053(10)	0.0107(10)	0.0059(5)	
	U_{33} (Å^2)	0.018(2)	0.021(2)	0.026(2)	0.029(3)	0.032(3)	0.035(2)	$= U_{11}$(Al)	
O1	$U_{11} = U_{22}$ (Å^2)	0.0031(3)	0.0053(4)	0.0074(4)	0.0079(4)	0.0093(4)	0.0134(4)	0.0032(8)	
	U_{33} (Å^2)	0.0112(7)	0.0080(10)	0.0140(10)	0.0166(10)	0.0210(11)	0.0243(11)	$= U_{11}$(O1)	
O2	z	0.16241(12)	0.16299(18)	0.16299(17)	0.16295(16)	0.16281(16)	0.16316(16)	0.1621(3)	0.1653
	$U_{11} = U_{22}$ (Å^2)	0.0094(4)	0.0137(5)	0.0173(5)	0.0210(6)	0.0249(6)	0.0297(6)	0.0057(8)	
	U_{33} (Å^2)	0.0088(9)	0.0124(10)	0.0111(10)	0.0108(9)	0.0126(10)	0.0188(10)	$= U_{11}$(O2)	
reliability factors in Rietveld analysis									
	R_{wp} (%)	5.966	6.675	6.406	5.855	5.447	4.897	4.062	
	GoF	2.309	2.490	2.275	2.033	1.822	1.661	1.918	
	R_B (%)	1.494	2.335	3.310	1.883	2.131	2.183	2.416	
	R_F (%)	0.740	1.326	1.632	0.964	1.367	1.231	1.056	

[a]Space group: tetragonal $I4/mmm$. La and Sr atoms are located at the same position: 0, 0, z. The Al atom is placed at 1/2, 1/2, 1/2. Equatorial O1 and apical O2 oxygen atoms are located at 1/2, 0, 1/2 and 0, 0, z, respectively. The number in parentheses is the estimated standard deviation of the last digit. $g(X)$: occupancy factor of X atom. g(La) = g(Sr) = 1/2, g(Al) = g(O1) = g(O2) = 1.0. $U_{iso}(X)$: isotropic atomic displacement parameter of X atom. $U_{ij}(X)$: anisotropic atomic displacement parameter of X atom. $U_{12}(X) = U_{23}(X) = U_{31}(X) = 0$, and $U_{22}(X) = U_{11}(X)$. [b]Space group: triclinic $P1$. All theoretical unit-cell parameters and atomic coordinates were in good agreement with experimental values.

Table 2. Refined Crystallographic Parameters and Reliability Factors in the Rietveld Analysis of Sr_2TiO_4 at Different Temperatures[a] and Crystallographic Parameters Optimized by DFT Calculations[b]

method		neutron diffraction through the Echidna diffractometer[a]						synchrotron[a]	DFT[b]
temperature		298 K	473 K	673 K	873 K	1073 K	1273 K	300 K	
	$a = b$ (Å)	3.88656(7)	3.89494(5)	3.90408(6)	3.91289(7)	3.92271(7)	3.93297(8)	3.88340(2)	3.92579
	c (Å)	12.5975(4)	12.6263(3)	12.6566(3)	12.6866(3)	12.7196(3)	12.7535(4)	12.58630(10)	12.67732
Sr	z	0.35377(18)	0.35383(13)	0.35371(14)	0.35361(16)	0.35375(18)	0.35323(19)	0.35410(4)	0.3547
	$U_{11} = U_{22}$ (Å^2)	0.0064(7)	0.0115(6)	0.0174(6)	0.0222(7)	0.0274(8)	0.0317(8)	0.00654(11)	
	U_{33} (Å^2)	0.0073(12)	0.0089(9)	0.0119(10)	0.0160(11)	0.0213(12)	0.0276(13)	$= U_{11}$(Sr)	
Ti	U_{iso} (Å^2)	0.0012(11)	0.0056(9)	0.0090(9)	0.0112(10)	0.0135(10)	0.0189(11)	0.0036(3)	
O1	$U_{11} = U_{22}$ (Å^2)	0.0039(6)	0.0064(5)	0.0103(5)	0.0144(6)	0.0178(7)	0.0224(7)	0.0075(7)	
	U_{33} (Å^2)	0.0089(13)	0.0140(10)	0.0212(11)	0.0260(11)	0.0295(12)	0.0377(13)	$= U_{11}$(O1)	
O2	z	0.1572(2)	0.15666(16)	0.1568(16)	0.15649(18)	0.1566(2)	0.1558(2)	0.1568(2)	0.1582
	$U_{11} = U_{22}$ (Å^2)	0.0075(9)	0.0131(7)	0.0208(8)	0.0276(10)	0.0309(11)	0.0403(12)	0.0078(7)	
	U_{33} (Å^2)	0.0072(13)	0.0066(10)	0.0074(11)	0.0093(13)	0.0166(14)	0.0225(15)	$= U_{11}$(O2)	
reliability factors in Rietveld analysis									
	R_{wp} (%)	8.260	6.280	5.924	5.749	5.397	4.782	2.112	
	GoF	1.247	1.787	1.745	1.663	1.494	1.389	1.488	
	R_B (%)	2.474	2.338	1.728	1.730	1.966	0.971	1.370	
	R_F (%)	1.368	1.337	0.979	1.007	1.349	0.720	0.592	

[a]Space group: tetragonal $I4/mmm$. Sr atom is located at 0, 0, z. The Ti atom is placed at 1/2, 1/2, 1/2. Equatorial O1 and apical O2 oxygen atoms are located at 1/2, 0, 1/2 and 0, 0, z, respectively. The number in parentheses is the estimated standard deviation of the last digit. $g(X)$: occupancy factor of X atom. g(Sr) = g(Ti) = g(O1) = g(O2) = 1.0. $U_{iso}(X)$: isotropic atomic displacement parameter of X atom. $U_{ij}(X)$: anisotropic atomic displacement parameter of X atom. $U_{12}(X) = U_{23}(X) = U_{31}(X) = 0$, and $U_{22}(X) = U_{11}(X)$. [b]Space group: triclinic $P1$. All the theoretical unit-cell parameters and atomic coordinates were in good agreement with experimental values.

$$\alpha_a \equiv [a(1273) - a(298)]/a(298)/975$$

$$\alpha_c \equiv [c(1273) - c(298)]/c(298)/975 \quad (3)$$

For $LaSrAlO_4$, the average TEC along the c-axis [$\alpha_c = 17.75(3) \times 10^{-6}$ K^{-1}] is 1.882(4) times higher than that along the a-axis [$\alpha_a = 9.430(18) \times 10^{-6}$ K^{-1}] (Table 3). For Sr_2TiO_4, the average TEC along the c-axis [$\alpha_c = 12.70(4) \times 10^{-6}$ K^{-1}] is nearly equal to that along the a-axis [$\alpha_a = 12.25(3) \times 10^{-6}$ K^{-1}, $\alpha_c = 1.037(4)\alpha_a$]. These results indicate that the thermal expansion of $LaSrAlO_4$ is anisotropic ($\alpha_c \gg \alpha_a$), whereas that of Sr_2TiO_4 is isotropic ($\alpha_c \approx \alpha_a$), which is consistent with the literature.[22,23,30,31]

Next, we investigated the temperature dependence of interatomic distances of $LaSrAlO_4$ and Sr_2TiO_4 to discuss the atomic-scale structural origin of the thermal expansion anisotropy. To simplify the following discussion, we examined only B−(equatorial oxygen atom O1), B−(apical oxygen atom

DOI: 10.1021/acs.inorgchem.5b00102
Inorg. Chem. 2015, 54, 3896−3904

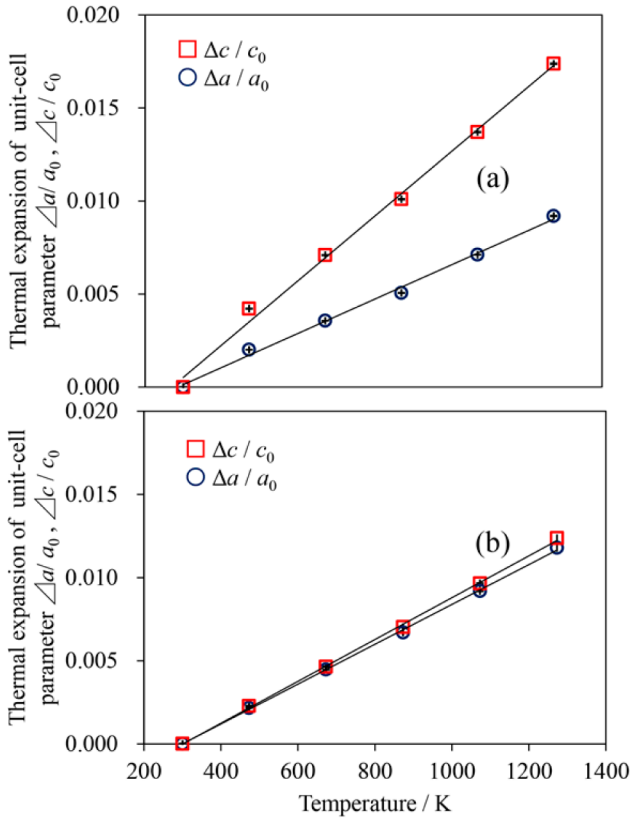

Figure 4. Thermal expansion of unit-cell parameters $\Delta a/a_0$ and $\Delta c/c_0$ of (a) $LaSrAlO_4$ and (b) Sr_2TiO_4.

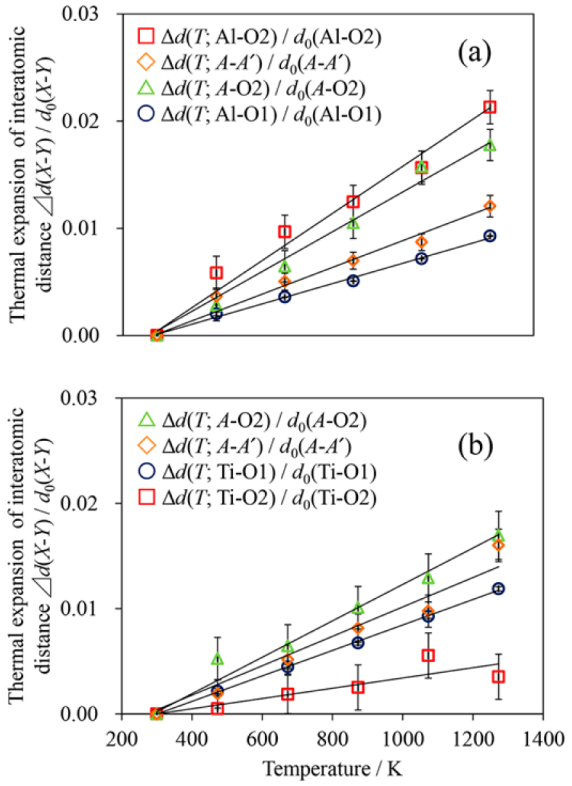

Figure 5. Thermal expansion of interatomic distances between X and Y atoms of (a) $LaSrAlO_4$ and (b) Sr_2TiO_4 ($\Delta d(T; X{-}Y)/d_0(X{-}Y)$, which is defined as $\Delta d(T; X{-}Y)/d_0(X{-}Y) \equiv [d(T; X{-}Y) - d(T_0; X{-}Y)]/d(T_0; X{-}Y)$).

O2), A−O2, and A−A' atomic pairs of A_2BO_4 (A = La, Sr; B = Al, Ti) (Figure 1). The thermal expansion of the interatomic distance between X and Y atoms, $\Delta d(X{-}Y)/d_0(X{-}Y) \equiv [d(T; X{-}Y) - d(T_0; X{-}Y)]/d(T_0; X{-}Y)$, increases with temperature (Figure 5), where $d(T; X{-}Y)$ is the interatomic distance between X and Y atoms at temperature T. The average thermal expansion coefficient of interatomic distance between X and Y atoms from 298 to 1273 K, $\alpha(X{-}Y)$, is defined as

$$\alpha(X{-}Y) \equiv [d(T; X{-}Y) - d(T_0; X{-}Y)]/d(T_0; X{-}Y)/(T - T_0)$$
$$= [d(1273; X{-}Y) - d(298; X{-}Y)]/d(298; X{-}Y)/975 \quad (4)$$

where T = 1273 K and T_0 = 298 K. For $LaSrAlO_4$, the average TECs of B−(equatorial oxygen atom O1), B−(apical oxygen atom O2), A−O2, and A−A' interatomic distances were estimated to be 9.43(2), 22.7(17), 17.5(15), and 12.5(10) ($\times 10^{-6}$ K^{-1}), respectively. For Sr_2TiO_4, the average TECs of B−O1, B−O2, A−O2, and A−A' interatomic distances were 12.25(3), 3(2), 17(2), and 16.7(16) ($\times 10^{-6}$ K^{-1}), respectively. There is a large difference between the average TECs of B−O2 interatomic distance of $LaSrAlO_4$ and Sr_2TiO_4, whereas the other TECs (B−O1, A−O2, and A−A') are not very different between $LaSrAlO_4$ and Sr_2TiO_4. This fact indicates the importance of B−O to understand the structural origin of the anisotropic and isotropic thermal expansion of $LaSrAlO_4$ and Sr_2TiO_4. Compared to the B−O1 interatomic distance, the B−O2 interatomic distance has a higher TEC for $LaSrAlO_4$ and lower TEC for Sr_2TiO_4, which would lead to anisotropic and isotropic thermal expansions for $LaSrAlO_4$ and Sr_2TiO_4, respectively. The ratio of TEC of interatomic distance $\alpha(B{-}O2)/\alpha(B{-}O1)$ (0.25(18)) for Sr_2TiO_4 is much smaller than that of $\alpha(B{-}O2)/\alpha(B{-}O1)$ (2.41(18)) for $LaSrAlO_4$.

As shown in Figure 1, the unit-cell parameters $a(T)$ and $c(T)$ are expressed by functions of interatomic distances $d(T; X{-}Y)$,

$$a(T) = 2d(T; B{-}O1)$$
$$c(T) = 2d(T; B{-}O2) + 2d(T; A{-}O2) + d(T; A{-}A') \quad (5)$$

Table 3. Average Thermal Expansion Coefficients (TECs) along the *a*-axis, α_a, and *c*-axis, α_c, and Average Linear TECs α_L of $LaSrAlO_4$ and Sr_2TiO_4 in Different Temperature Ranges[a]

	$LaSrAlO_4$			Sr_2TiO_4		
	298−873 K	298−1073 K	298−1273 K	298−873 K	298−1073 K	298−1273 K
α_a ($\times 10^{-6}$ K^{-1})	8.879(15)	9.246(15)	9.430(18)	11.78(4)	12.00(3)	12.25(3)
α_c ($\times 10^{-6}$ K^{-1})	17.61(3)	17.72(3)	17.75(3)	12.30(7)	12.50(5)	12.70(4)
α_L ($\times 10^{-6}$ K^{-1})	11.86(3)	12.18(4)	12.34(4)	12.04(3)	12.28(2)	12.55(2)

[a] $\alpha_a \equiv (a(T) - a(T_0))/a(T_0)/(T - T_0)$, $\alpha_c \equiv (c(T) - c(T_0))/c(T_0)/(T - T_0)$, $\alpha_L \equiv (v(T) - v(T_0))/v(T_0)/(T - T_0)$ where $v(T) \equiv [a(T)\ a(T)\ c(T)]^{1/3}$.

DOI: 10.1021/acs.inorgchem.5b00102
Inorg. Chem. 2015, 54, 3896−3904

Using eqs 3−5, the average TECs along the *a*- and *c*-axes are described by functions of average TECs of interatomic distances[28,29]

$$\alpha_a = \alpha(B{-}O1),$$

$$\alpha_c = 2d(T_0;\ B{-}O2)\cdot\alpha(B{-}O2)/c(T_0)+2d(T_0;\ A{-}O2)\cdot \alpha(A{-}O2)/c(T_0)+d(T_0;\ A{-}A')\cdot\alpha(A{-}A')/c(T_0)$$

Thus, the contributions of B−O2, A−O2, and A−A' to α_c are $2d(T_0;\ B{-}O2)\cdot\alpha(B{-}O2)/c(T_0)$, $2d(T_0;\ A{-}O2)\cdot\alpha(A{-}O2)/c(T_0)$, and $d(T_0;\ A{-}A')\cdot\alpha(A{-}A')/c(T_0)$, respectively. For $LaSrAlO_4$, the contributions of the average TECs of B−O2, A−O2, and A−A' interatomic distances to α_c were estimated to be 42(3), 39(3), and 20(2)%, respectively (Figure 6a). In

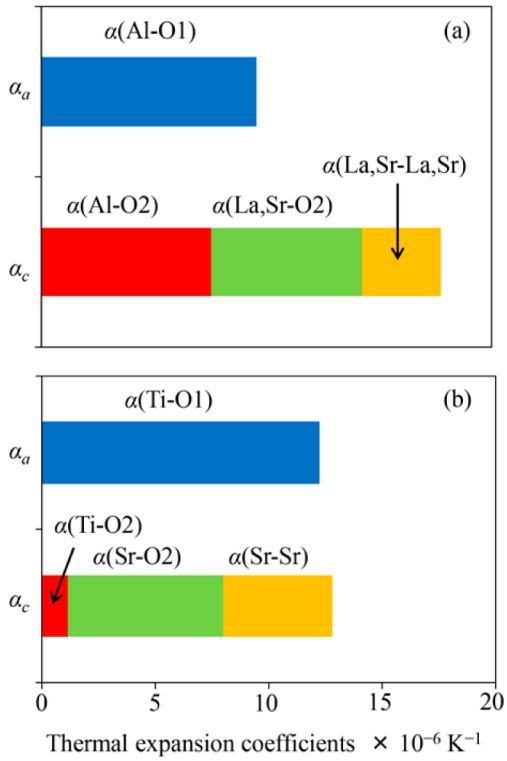

Figure 6. Average thermal expansion coefficients (TECs) along the *a*- and *c*-axes (α_a and α_c) between 298 and 1273 K of (a) $LaSrAlO_4$ and (b) Sr_2TiO_4. Contributions of average TECs of interatomic distances $\alpha(X{-}Y)$ to α_c.

contrast, for Sr_2TiO_4, the contributions of the average TECs of B−O2, A−O2, and A−A' interatomic distances to α_c were calculated to be 8(5), 54(7), and 38(4)%, respectively (Figure 6b). These results indicate that α_c being higher than α_a for $LaSrAlO_4$ is mainly attributable to the higher TEC of the B−O2 bond [$\alpha(B{-}O2) = 22.7(17) \times 10^{-6}\ K^{-1}$] compared with that of the B−O1 bond [$\alpha(B{-}O1) = 9.43(2) \times 10^{-6}\ K^{-1}$], whereas the smaller TEC of the B−O2 bond [$\alpha(B{-}O2) = 3(2) \times 10^{-6}\ K^{-1}$] compared with that of the B−O1 bond [$\alpha(B{-}O1) = 12.25(3) \times 10^{-6}\ K^{-1}$] leads to isotropic thermal expansion of the unit cell parameters of Sr_2TiO_4.

Next, we explain the anisotropic thermal expansion of $LaSrAlO_4$ and the isotropic behavior of Sr_2TiO_4 through electron-density distributions. Figure 7a and b show the electron-density distributions obtained by the MEM analysis of synchrotron X-ray powder diffraction data of $LaSrAlO_4$ and

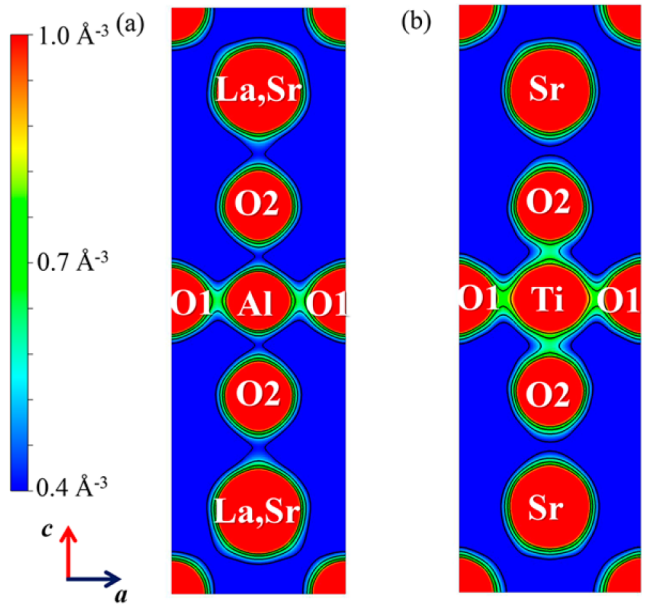

Figure 7. Experimental electron-density distributions on the *ac* plane at $y = 0$ of (a) $LaSrAlO_4$ and (b) Sr_2TiO_4 ($-1/2 \le x \le 1/2$, $-1/2 \le z \le 1/2$).

Sr_2TiO_4, respectively, at 300 K. These experimental electron-density distributions are consistent with theoretical ones obtained by DFT calculations (Figure 8).

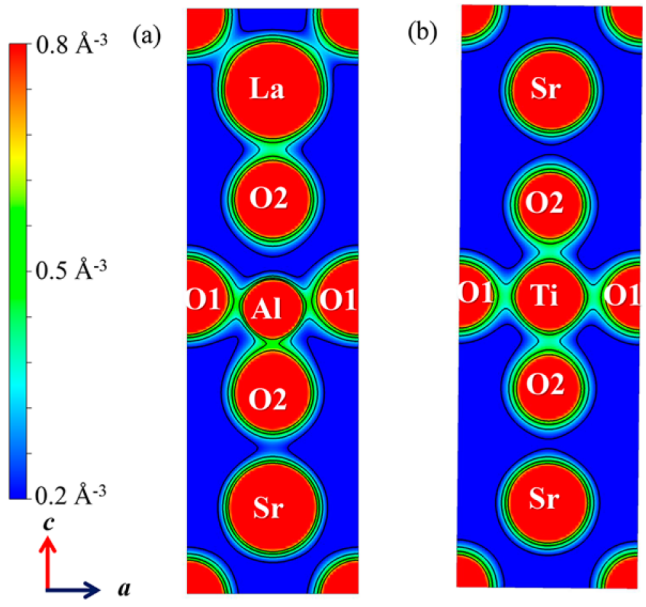

Figure 8. Theoretical electron-density distributions on the *ac* plane at $y = 0$ of (a) $LaSrAlO_4$ and (b) Sr_2TiO_4 ($-1/2 \le x \le 1/2$, $-1/2 \le z \le 1/2$). The distribution does not have reflection symmetry as the calculations were performed without imposing symmetry constraints in the *P*1 space group.

For $LaSrAlO_4$, the B−O2 distance (2.0535(16) Å) is longer than that of B−O1 (1.87832(3) Å) [$d(B{-}O2)/d(B{-}O1) = 1.0932(9) > 1$], and the minimum electron density (MED) at the B−O2 bond (0.40 $Å^{-3}$) is lower than that at B−O1 (0.64 $Å^{-3}$) [$\mathrm{MED}(B{-}O2)/\mathrm{MED}(B{-}O1) = 0.625 < 1$]. Thus, the bond force constant f of the B−O2 bond f (B−O2) would be lower than that of B−O1 [$f(B{-}O2)/f(B{-}O1) < 1$]. Because the

DOI: 10.1021/acs.inorgchem.5b00102
Inorg. Chem. 2015, 54, 3896−3904

TEC is proportional to f^{-1},[35] the TEC of the B−O2 bond is higher than that of B−O1 [$\alpha(B-O2)/\alpha(B-O1) = 2.41(18) > 1$]. These results indicate that the structural origin of anisotropic thermal expansion of $LaSrAlO_4$ [$\alpha_c/\alpha_a = 1.882(4) > 1$] is the longer and weaker B−O2 bond relative to that of B−O1. These results are similar to those of $CaErAlO_4$ and $CaYAlO_4$.[28,29]

For Sr_2TiO_4, the B−O2 distance (1.981(3) Å) is nearly equal to that of B−O1 (1.94328(4) Å); thus, the ratio of interatomic distance $d(B-O2)/d(B-O1)$ of Sr_2TiO_4 (1.0194(15)) is smaller than that of $LaSrAlO_4$ (1.0932(9)). Corresponding to the smaller ratio $d(B-O2)/d(B-O1)$ of Sr_2TiO_4 compared to that of $LaSrAlO_4$, the ratio of the minimum electron density $MED(B-O2)/MED(B-O1)$ in Sr_2TiO_4 (0.91) is higher than that of $LaSrAlO_4$ (0.625). Therefore, the ratio of the bond force constant $[f(B-O2)/f(B-O1)]$ of Sr_2TiO_4 would be higher than that of $LaSrAlO_4$, leading to a smaller ratio of TEC $\alpha(B-O2)/\alpha(B-O1)$ of Sr_2TiO_4 (0.25(18)) compared with that of $LaSrAlO_4$ (2.41(18)). Thus, the isotropic MED of B−O bonds in Sr_2TiO_4 [$MED(B-O2)/MED(B-O1) = 0.91$] is a factor of isotropic thermal expansion of Sr_2TiO_4 [$\alpha_c/\alpha_a = 1.037(4) \cong 1$] compared with $LaSrAlO_4$ [$MED(B-O2)/MED(B-O1) = 0.625$, $\alpha_c/\alpha_a = 1.882(4) > 1$].

Next, we discuss the anisotropic and isotropic thermal expansion of $LaSrAlO_4$ and Sr_2TiO_4 using a relation[35] between the thermal expansion coefficient and bond valence. We calculated the bond valence of B−O bonds by the relation[50,51] between bond valence, $BV(i-j)$, and bond length, $d(i-j)$.

$$BV(i-j) = \exp[(d_0(i-j) - d(i-j))/b]$$

where $d_0(i-j)$ and b (0.37) are empirically determined constants. For $LaSrAlO_4$ (B = Al), the bond valence of the B−O2 bond $BV(B-O2)$ estimated from the refined crystal parameters at 298 K is smaller than that of B−O1 [$BV(B-O2)/BV(B-O1) = 0.62 < 1$]. Using the approximate relationship between bond force constant $f(i-j)$ and bond valence $BV(i-j)$,

$$f(i-j) = \{k_0(8BV(i-j)/3)^{3/2}(1/b - 2/d(i-j))\}/d(i-j)^2 \quad (6)$$

where k_0 is Coulomb's constant,[52] we obtain the $f(B-O2)/f(B-O1)$ ratio in $LaSrAlO_4$. The calculated bond force constant of the B−O2 bond in $LaSrAlO_4$ is smaller than that of B−O1 [$f(B-O2)/f(B-O1) = 0.44 < 1$]. The thermal expansion coefficient of the i−j bond, $\alpha(i-j)$ is expressed by

$$\alpha(i-j) = 1.35k_B/\{f(i-j)\cdot d(i-j)\} \quad (7)$$

where k_B is Boltzmann's constant.[35] The TEC of the B−O2 bond calculated using eq 7, $f(B-O2)$, and $d(B-O2)$ is higher than the TEC of B−O1 [$\alpha(B-O2)/\alpha(B-O1) = 2.08 > 1$]. The calculated ratio 2.08 of $LaSrAlO_4$ is in good agreement with the present experimental data [$\alpha(B-O2)/\alpha(B-O1) = 2.41(18) > 1$]. Therefore, we conclude that the anisotropic thermal expansion of B−O bond lengths ($\alpha(B-O2)/\alpha(B-O1) > 1$) is ascribed to anisotropy in the B−O bond lengths ($d(B-O2)/d(B-O1) > 1$), which is due to the combination of the cation valences +3, +2, and +3 for La, Sr, and Al, respectively, as shown in relation 1. As discussed above (Figure 6), the anisotropic TEC of unit-cell parameters in $LaSrAlO_4$ [$\alpha_c/\alpha_a > 1$] is mainly attributable to the anisotropic TEC of B−O bonds [$\alpha(B-O2)/\alpha(B-O1) > 1$]. Thus, the combination of cation valences is essential for the anisotropy of B−O bond lengths and of the thermal expansion of unit-cell parameters of $LaSrAlO_4$.

Next, we discuss the origin of isotropic thermal expansion of Sr_2TiO_4 by the bond valence method. The B−O bond lengths in Sr_2TiO_4 (B = Ti) are isotropic compared to those in $LaSrAlO_4$ (B = Al). Thus, the ratio of the bond valence $BV(B-O2)/BV(B-O1)$ in Sr_2TiO_4 (0.90) estimated from the refined crystal parameters at 298 K is higher than that of $LaSrAlO_4$ (0.62). Using these values and eq 6, the ratio of the bond force constant $f(B-O2)/f(B-O1)$ in Sr_2TiO_4 is estimated to be 0.84, which is higher than that of $LaSrAlO_4$ (0.44). Thus, using eq 7, we obtain the relation that the TEC ratio $\alpha(B-O2)/\alpha(B-O1)$ of Sr_2TiO_4 is smaller than that of $LaSrAlO_4$, which is consistent with the experimental result that $\alpha(B-O2)/\alpha(B-O1)$ of Sr_2TiO_4 (0.25(18)) is smaller than that of $LaSrAlO_4$ (2.41(18)). Therefore, we conclude that the smaller thermal expansion ratio $\alpha(B-O2)/\alpha(B-O1)$ leading to the isotropic TEC [$\alpha_c/\alpha_a = 1.037(4) \cong 1$] of Sr_2TiO_4 is attributable to isotropy in the B−O bond lengths $d(B-O2)/d(B-O1)$ (≈ 1), which is due to the combination of the cation valences +2 and +4 for Sr and Ti, respectively, as shown in relation 2. Thus, the combination of cation valences +2 and +4 for Sr and Ti is essential for isotropy of the B−O bond lengths and for thermal expansion of the unit-cell parameters of Sr_2TiO_4.

The mean TECs, $\bar{\alpha}$, of K_2NiF_4-type A_2BO_4 oxides have been believed to be lower than the coefficients $\bar{\alpha}$ of the perovskite-type ABO_3 oxides of comparable cationic compositions ($\bar{\alpha}(A_2BO_4) < \bar{\alpha}(ABO_3)$).[53] However, the mean TEC $\bar{\alpha}$ of the present K_2NiF_4-type $LaSrAlO_4$ ($\bar{\alpha}(LaSrAlO_4) = (2\alpha_a + \alpha_c)/3 = 12.203(15) \times 10^{-6}$ K^{-1} (298−1273 K)) is higher than that of perovskite-type oxide with a similar composition $LaAlO_3$ ($\bar{\alpha}(LaAlO_3) = (\alpha_a + \alpha_b + \alpha_c)/3 = 10.77(11) \times 10^{-6}$ K^{-1} (300−1270 K)).[54] The $\bar{\alpha}$ of the present Sr_2TiO_4 ($\bar{\alpha}(Sr_2TiO_4) = (2\alpha_a + \alpha_c)/3 = 12.39(2) \times 10^{-6}$ K^{-1} (298−1273 K)) is also higher than that of perovskite-type oxide with a similar composition $SrTiO_3$ ($\bar{\alpha}(SrTiO_3) = \alpha_a = 10.80(8) \times 10^{-6}$ K^{-1} (300−1235 K)).[55] The same relation ($\bar{\alpha}(A_2BO_4) > \bar{\alpha}(ABO_3)$) is also valid for $CaErAlO_4$[28] and $CaYAlO_4$.[29] This discrepancy between our results ($\bar{\alpha}(A_2BO_4) > \bar{\alpha}(ABO_3)$) in this work and in refs 28 and 29 and the previous work ($\bar{\alpha}(A_2BO_4) < \bar{\alpha}(ABO_3)$)[53] is attributable to the chemical expansion in perovskite-type transition metal oxides ABO_3 in the literature:[56] the change of transition-metal-cation B^{n+} valence $n+$ (e.g., B = Fe and Co) and oxygen content $3-\delta$ in $ABO_{3-\delta}$ with temperature. On the contrary, $LaSrAlO_4$, $LaAlO_3$, Sr_2TiO_4, and $SrTiO_3$ do not exhibit chemical expansion. The inequalities, $\bar{\alpha}(LaSrAlO_4) > \bar{\alpha}(LaAlO_3)$ and $\bar{\alpha}(Sr_2TiO_4) > \bar{\alpha}(SrTiO_3)$ are attributable to the higher TEC of the SrO unit. In fact, the rock-salt-type SrO has a higher TEC: $\alpha(SrO) = 13.92 \times 10^{-6}$ K^{-1} (298−1273 K).[57] The "average" TEC of $LaAlO_3$ and SrO ($[\bar{\alpha}(LaAlO_3) + \alpha(SrO)]/2 = 12.27 \times 10^{-6}$ K^{-1}) agrees with $\bar{\alpha}(LaSrAlO_4)$ ($12.203(15) \times 10^{-6}$ K^{-1}). The "average" TEC of $SrTiO_3$ and SrO ($[\bar{\alpha}(SrTiO_3) + \alpha(SrO)]/2 = 12.28 \times 10^{-6}$ K^{-1}) agrees with $\bar{\alpha}(Sr_2TiO_4)$ ($12.39(2) \times 10^{-6}$ K^{-1}).

4. CONCLUSIONS

We have investigated the crystal structure, thermal expansion, and electron-density distribution of K_2NiF_4-type $LaSrAlO_4$ and Sr_2TiO_4 through neutron powder diffraction experiments between 298 and 1273 K, synchrotron X-ray diffraction measurements at 300 K, and ab initio electronic calculations. The thermal expansion coefficient along the c-axis being higher than that along the a-axis of $LaSrAlO_4$ [$\alpha_c(LaSrAlO_4)/\alpha_a(LaSrAlO_4) > 1$] is mainly ascribed to the TEC of interatomic distance between Al and apical oxygen atom O2, $\alpha(Al-O2)$, being higher than the TEC of interatomic distance between Al and equatorial oxygen atom O1, $\alpha(Al-O1)$ [$\alpha(Al-O2)/\alpha(Al-O1) > 1$]. The higher $\alpha(Al-O2)$ is attributed to the Al−O2 bond

DOI: 10.1021/acs.inorgchem.5b00102
Inorg. Chem. 2015, 54, 3896−3904

being longer and weaker than the Al−O1 bond. The bond valence and the minimum electron density of Al−O2 are smaller than those of Al−O1 [BV(Al−O2)/BV(Al−O1) < 1, MED(Al−O2)/MED(Al−O1) < 1]. The ratios of BV and MED for Sr_2TiO_4 are higher than those of $LaSrAlO_4$ [BV(Ti−O2)/BV(Ti−O1) > BV(Al−O2)/BV(Al−O1), MED(Ti−O2)/MED(Ti−O1) > MED(Al−O2)/MED(Al−O1)]. Thus, the ratio of TEC of interatomic distance α(Ti−O2)/α(Ti−O1) is smaller than that of α(Al−O2)/α(Al−O1) [α(Ti−O2)/α(Ti−O1) < α(Al−O2)/α(Al−O1)], leading to the smaller ratio of TEC of the cell parameters [$\alpha_c(Sr_2TiO_4)/\alpha_a(Sr_2TiO_4) < \alpha_c(LaSrAlO_4)/\alpha_a(LaSrAlO_4)$]. These results indicate that anisotropic thermal expansion of K_2NiF_4-type oxide A_2BO_4 is strongly influenced by anisotropy of the B−O bonds (B = Al, Ti). The present study has also indicated that due to the ratio of interatomic distance $d(B-O2)/d(B-O1)$ of $A_2^{2.5+}B^{3+}O_4$ being higher than that of $A_2^{2+}B^{4+}O_4$, $A_2^{2.5+}B^{3+}O_4$ compounds such as $LaSrAlO_4$ have a higher thermal expansion coefficient, $\alpha(B-O2)$, and $A_2^{2+}B^{4+}O_4$ materials such as Sr_2TiO_4 exhibit smaller $\alpha(B-O2)$, leading to the anisotropic thermal expansion of $A_2^{2.5+}B^{3+}O_4$ compounds and isotropic thermal expansion of $A_2^{2+}B^{4+}O_4$ materials. In contrast to a previous report [$\overline{\alpha}(A_2BO_4) < \overline{\alpha}(ABO_3)$], the "true" TEC of A_2BO_4 is higher than that of ABO_3 [$\overline{\alpha}(A_2BO_4) > \overline{\alpha}(ABO_3)$] for $LaSrAlO_4$, Sr_2TiO_4, $CaErAlO_4$, and $CaYAlO_4$.

■ ASSOCIATED CONTENT

Supporting Information

Refined occupancy factors in the preliminary Rietveld analyses, thermogravimetric analysis (TGA) data, and temperature dependence of the unit-cell parameters. This material is available free of charge via the Internet at http://pubs.acs.org.

■ AUTHOR INFORMATION

Corresponding Author

*E-mail: yashima@cms.titech.ac.jp.

Author Contributions

The manuscript was written mainly by K.K., M.Y., and K.F. K.K. prepared the samples. M.Y. designed the research project. All authors contributed to the neutron experiments and/or their planning.

Funding

This work was supported by a Grant-in-Aid for Scientific Research (KAKENHI 24850009, 24246107, 24226016, and 25630365) from the Ministry of Education, Culture, Sports, Science and Technology of Japan. Travel costs for Echidna neutron experiments of K.K., K.O., K.H., and S.Y. were partially supported by the Institute for Solid State Physics, The University of Tokyo (12725, 13679, 14643, and 14657), Japan Atomic Energy Agency, Tokai, Japan.

Notes

The authors declare no competing financial interest.

■ ACKNOWLEDGMENTS

We thank Dr. K. Osaka, Prof. T. Ishigaki, and Prof. A. Hoshikawa for assistance with the synchrotron and neutron diffraction experiments. The synchrotron experiments were carried out on BL19B2 at SPring-8 (2013B1718, 2014A1510, and 2014B1660) and on BL-4B2 at PF (2011G640, 2013G053, and 2013G216). The neutron diffraction measurements were performed with approval (Echidna: 2696, 3209; iMATERIA: 2013A0136, 2013B0178, 2014PM0003, 2014AM0011, 2014B0114; SuperHRPD: 2013B0198, 2014B0233). We thank the Center for Materials Analysis at O-okayama of Tokyo Institute of Technology for the ICP-OES measurements.

■ REFERENCES

(1) Shimura, T.; Suzuki, K.; Iwahara, H. *Solid State Ionics* **1999**, *125*, 313−318.
(2) Wang, X. L.; Takayama-Muromachi, E. *Phys. Rev. B: Condens. Matter Mater. Phys.* **2005**, *72*, 064401.
(3) Kharton, V. V.; Tsipis, E. V.; Naumovich, E. N.; Thursfield, A.; Patrakeev, M. V.; Kolotygin, V. A.; Waerenborgh, J. C.; Metcalfe, I. S. *J. Solid State Chem.* **2008**, *181*, 1425−1433.
(4) Mizuno, N.; Yamato, M.; Tanaka, M.; Misono, M. *Chem. Mater.* **1989**, *1*, 232−236.
(5) Kharton, V. V.; Tsipis, E. V.; Yaremchenko, A. A.; Frade, J. R. *Solid State Ionics* **2004**, *166*, 327−337.
(6) Amow, G.; Skinner, S. J. *J. Solid State Electrochem.* **2006**, *10*, 538−546.
(7) (a) Ishihara, T.; Nakashima, K.; Okada, S.; Enoki, M.; Matsumoto, H. *Solid State Ionics* **2008**, *179*, 1367−1371. (b) Sirikanda, N.; Matsumoto, H.; Ishihara, T. *Solid State Ionics* **2011**, *192*, 599−601.
(8) Aguadero, A.; Alonso, J. A.; Escudero, M. J.; Daza, L. *Solid State Ionics* **2008**, *179*, 393−400.
(9) Yashima, M.; Enoki, M.; Wakita, T.; Ali, R.; Matsushita, Y.; Izumi, F.; Ishihara, T. *J. Am. Chem. Soc.* **2008**, *130*, 2762−2763.
(10) Yashima, M.; Sirikanda, N.; Ishihara, T. *J. Am. Chem. Soc.* **2010**, *132*, 2385−2392.
(11) Zhao, H.; Li, Q.; Sun, L. *Sci. China: Chem.* **2011**, *54*, 898−910.
(12) Bednorz, J. G.; Müller, K. A. *Phys. Rev. B: Condens. Matter Mater. Phys.* **1986**, *64*, 189−193.
(13) Phillips, J. M. *J. Appl. Phys.* **1996**, *79*, 1829−1848.
(14) Novosselov, A. V.; Zimina, G. V.; Filaretov, A. A.; Shlyakhtin, O. A.; Komissarova, L. N.; Pajaczkowska, A. *Mater. Res. Bull.* **2001**, *36*, 1789−1798.
(15) Zhu, Z.; Zeng, H.; Li, J.; You, Z.; Wang, Y.; Huang, Z.; Tu, C. *CrystEngComm* **2012**, *14*, 7423−7427.
(16) Tietz, F. *Ionics* **1999**, *5*, 129−139.
(17) Bishop, S. R.; Duncan, K. L.; Wachsman, E. D. *ECS Trans.* **2006**, *1* (7), 13−21.
(18) Atkinson, A.; Ramos, T. M. G. M. *Solid State Ionics* **2000**, *129*, 259−269.
(19) Bishop, S. R.; Marrocchelli, D.; Chatzichristodoulou, C.; Perry, N. H.; Mogensen, M. B.; Tuller, H. L.; Wachsman, E. D. *Annu. Rev. Mater. Res.* **2014**, *44*, 205−239.
(20) Hashimoto, T.; Fueki, K.; Kishi, A.; Azumi, T.; Koinuma, H. *Jpn. J. Appl. Phys.* **1988**, *27*, L214−L216.
(21) Kharton, V. V.; Kovalevsky, A. V.; Avdeev, M.; Tsipis, E. V.; Patrakeev, M. V.; Yaremchenko, A. A.; Naumovich, E. N.; Frade, J. R. *Chem. Mater.* **2007**, *19*, 2027−2033.
(22) Byszewski, P.; Domagała, J.; Fink-Finowicki, J.; Pajaczkowska, A. *Mater. Res. Bull.* **1992**, *27*, 483−490.
(23) Raj, E. S.; Skinner, S. J.; Kilner, J. A. *Solid State Sci.* **2004**, *6*, 825−829.
(24) Skinner, S. J. *Solid State Sci.* **2003**, *5*, 419−426.
(25) Jennings, A. J.; Skinner, S. J. *Solid State Ionics* **2002**, *152−153*, 663−667.
(26) Yashima, M.; Yamada, H.; Nuansaeng, S.; Ishihara, T. *Chem. Mater.* **2012**, *24*, 4100−4113.
(27) Munnings, C. N.; Skinner, S. J.; Amow, G.; Whitfield, P. S.; Davidson, I. J. *Solid State Ionics* **2006**, *177*, 1849−1853.
(28) Omoto, K.; Yashima, M.; Hester, J. R. *Chem. Lett.* **2014**, *43*, 515−517.
(29) Omoto, K.; Yashima, M. *Appl. Phys. Express* **2014**, *7*, 037301.
(30) Galasso, F.; Darby, W. *J. Phys. Chem.* **1962**, *66*, 1318−1320.
(31) Assabaa-Boultif, R.; Marchand, R.; Laurent, Y.; Videau, J.-J. *Mater. Res. Bull.* **1994**, *29*, 667−672.
(32) Fu, W. T.; Visser, D.; Knight, K. S.; IJdo, D. J. W. *J. Solid State Chem.* **2004**, *177*, 4081−4086.

DOI: 10.1021/acs.inorgchem.5b00102
Inorg. Chem. 2015, 54, 3896−3904

(33) Yashima, M. *J. Am. Ceram. Soc.* **2002**, *85*, 2925−2930.
(34) (a) Yashima, M. *Solid State Ionics* **2008**, *179*, 797−803. (b) Yashima, M.; Ali, R. *Solid State Ionics* **2009**, *180*, 120−126. (c) Yashima, M. *J. Ceram. Soc. Jpn.* **2009**, *117*, 1055−1059. (d) Fujii, K.; Esaki, Y.; Omoto, K.; Yashima, M.; Hoshikawa, A.; Ishigaki, T.; Hester, J. R. *Chem. Mater.* **2014**, *26*, 2488−2491.
(35) Brown, I. D.; Dabkowski, A.; McCleary, A. *Acta Crystallogr., Sect. B: Struct. Sci.* **1997**, *53*, 750−761.
(36) Liu, X.; Wang, H.; Lavina, B.; Tu, B.; Wang, W.; Fu, Z. *Inorg. Chem.* **2014**, *53*, 5986−5992.
(37) Liss, K. -D.; Hunter, B.; Hagen, M.; Noakes, T.; Kennedy, S. *Phys. B* **2006**, *385*, 1010−1012.
(38) Torii, S.; Yonemura, M.; Panca Putra, T. Y. S.; Zhang, J.; Miao, P.; Muroya, T.; Tomiyasu, R.; Morishima, T.; Sato, S.; Sagehashi, H.; Noda, Y.; Kamiyama, T. *J. Phys. Soc. Jpn.* **2011**, *80*, SB020.
(39) Ishigaki, T.; Hoshikawa, A.; Yonemura, M.; Morishima, T.; Kamiyama, T.; Oishi, R.; Aizawa, K.; Sakuma, T.; Tomota, Y.; Arai, M.; Hayashi, M.; Ebata, K.; Takano, Y.; Komatsuzaki, K.; Asano, H.; Takano, Y.; Kasao, T. *Nucl. Instrum. Methods Phys. Res., Sect. A* **2009**, *600*, 189−191.
(40) BL19B2 Outline. http://www.spring8.or.jp/wkg/BL19B2/instrument/lang-en/INS-0000000300/instrument_summary_view, SPring-8 Website.
(41) Izumi, F.; Momma, K. *Solid State Phenom.* **2007**, *130*, 15−20.
(42) Oishi, R.; Yonemura, M.; Nishimaki, Y.; Torii, S.; Hoshikawa, A.; Ishigaki, T.; Morishima, T.; Mori, K.; Kamiyama, T. *Nucl. Instrum. Methods Phys. Res., Sect. A* **2009**, *600*, 94−96.
(43) Momma, K.; Ikeda, T.; Belik, A. A.; Izumi, F. *Powder Diffr.* **2013**, *28*, 184−193.
(44) Momma, K.; Izumi, F. *J. Appl. Crystallogr.* **2011**, *44*, 1272−1276.
(45) Kresse, G.; Joubert, D. *Phys. Rev. B: Condens. Matter Mater. Phys.* **1999**, *59*, 1758−1775.
(46) Tealdi, C.; Ferrara, C.; Malavasi, L.; Mustarelli, P.; Ritter, C.; Spinella, A.; Massiot, D.; Florian, P. *J. Mater. Chem.* **2012**, *22*, 10488−10495.
(47) Miwa, K.; Kagomiya, I.; Ohsato, H.; Sakai, H.; Maeda, Y. *J. Eur. Ceram. Soc.* **2007**, *27*, 4287−4290.
(48) The $d(B{-}O2)/d(B{-}O1)$ values were calculated using the experimental data compiled in ref 49.
(49) Benabbas, A. *Acta Crystallogr., Sect. B: Struct. Sci.* **2006**, *62*, 9−15.
(50) Brown, I. D.; Altermatt, D. *Acta Crystallogr., Sect. B: Struct. Sci.* **1985**, *41*, 244−247.
(51) Brese, N. E.; O'Keeffe, M. *Acta Crystallogr. B* **1991**, *47*, 192−197.
(52) Brown, I. D.; Klages, P.; Skowron, A. *Acta Crystallogr., Sect. B: Struct. Sci.* **2003**, *59*, 439−448.
(53) Al Daroukh, M.; Vashook, V. V.; Ullmann, H.; Tietz, F.; Arual Raj, I. *Solid State Ionics* **2003**, *158*, 141−150.
(54) Hayward, S. A.; Morrison, F. D.; Redfern, S. A. T.; Salje, E. K. H.; Scott, J. F.; Knight, K. S.; Tarantino, S.; Glazer, A. M.; Shuvaeva, V.; Daniel, P.; Zhang, M.; Carpenter, M. A. *Phys. Rev. B: Condens. Matter Mater. Phys.* **2005**, *72*, 054110.
(55) Ligny, D. D.; Richet, P. *Phys. Rev. B: Condens. Matter Mater. Phys.* **1996**, *53*, 3013−3022.
(56) Chen, X.; Yu, J.; Adler, S. B. *Chem. Mater.* **2005**, *17*, 4537−4546.
(57) Touloukian, Y. S.; Kirby, R. K.; Taylor, R. E.; Lee, T. Y. R. Thermal Expansion: Nonmetallic Solids. *Thermophysical Properties of Matter*; Plenum Pub. Co.: New York, 1977; Vol. *13*, pp 372−373.

DOI: 10.1021/acs.inorgchem.5b00102
Inorg. Chem. 2015, 54, 3896−3904